Journal of Thermal Analysis, Vol. 37 (1991) 2189-2203

THERMAL PROPERTIES OF CHALCOGENIDE-HALIDE GLASSES IN THE SYSTEM: Ge-S-I

A. B. Seddon and M. A. Hemingway

SCHOOL OF MATERIALS, UNIVERSITY OF SHEFFIELD, SHEFFIELD S10 2TZ, U.K.

Chalcogenide-halide glasses in the series $[Ge_{0.3}S_{0.7}]_{100-x}I_x$ where $0 \leq x \leq 30$ have been prepared and have potential applications as short length infrared optical fibres. As x is increased the expansion coefficient increases, in addition the glass transformation temperature and onset temperature of mass loss both decrease as determined by differential scanning calorimetry and thermogravimetry, respectively. Melt viscosities in the range 10^7–$10^{10.7}$ Pa s have been determined via penetration viscometry and isoviscous points are at lower temperatures as x increases. These results have been discussed in relation to known structural information and the fragility of the melts has been compared. Predicted fibre drawing temperatures tend to lie close to the onset of mass loss.

Introduction

The compositions of most of the container and flat glassware manufactured in bulk are based upon the ternary system $Na_2O \cdot CaO \cdot SiO_2$. Glass compositions based on successively heavier members than oxygen of group VI of the Periodic Table i.e. sulphur, selenium, and tellurium (in conjunction with one or more of Ge, As, P, Si, Sb, etc.) tend to be increasingly infrared transparent and are known as the chalcogenide glasses [1].

The first of a range of chalcogenide glasses to be commercially exploited was arsenic trisulphide which was developed for passive, bulk optical components for the mid-infrared in the 1950s. Since the early 1980s various infrared transmitting glasses have received attention as potential ultralow loss, telecommunication optical fibres to replace silica [2]. Chalcogenide optical fibres such as germanium sulphide have been investigated [3]. Much lower

* Present address: the Health and Safety Executive, RLSD, Broad Lane, Sheffield S3 7HQ, U.K.

John Wiley & Sons, Limited, Chichester
Akadémiai Kiadó, Budapest

optical losses have been attained for the multicomponent heavy metal fluoride glasses such as $ZrF_4 \cdot BaF_2 \cdot LaF_3 \cdot AlF_3 \cdot NaF$ (Acronym ZBLAN) [4, 5] but, so far, the losses achieved have not matched those of silica, hence ruling out long haul applications for the time being. Despite this, short-length fluoride or chalcogenide fibres have a number of potential applications including infrared sensing and laser power transmission. In addition, Nasu and Mackenzie [6] have predicted a high optical nonlinearity for the chalcogenides, possibly making them of use for optical fibre switching devices.

Chalcogenide-halide glasses [7] are formed by inclusion of a halogen in the chalcogenide compositions and have similar potential uses, but are less well characterised. One example is the germanium sulphide iodide system, whose glass forming region was originally mapped out by Dembrovskii *et al.* [8]. Sanghera *et al.* have recently reviewed glass properties [9] and carried out structural determinations *via* vibrational spectroscopy. The purpose of the current paper is to investigate thermal properties of the Ge-S-I system which are pertinent to optical fibre fabrication and to relate the results to known glass structural information.

For germanium sulphide glasses, a slight excess of sulphur over the stoichiometric ratio of S:Ge = 2:1 is claimed to enhance the glass forming ability [10]. Thus, throughout this work a base glass composition of $GeS_{2.3}$ was employed, as suggested by Savage [11] and the thermal behaviour of the compositional series $[Ge_{0.3}S_{0.7}]_{100-x}I_x$ as x increases was investigated.

Experimental

Glass batching and melting

Glasses were melted in a sealed system because of the potentially high vapour pressure exhibited by the sulphur and iodine batch components as the temperature is raised. Melting ampoules of silica were fabricated from Heraeus HSQ and directly prior to batching were rinsed in deionised water, dried at 100°C and vacuum baked at 10^{-5} torr/950°C (1 torr = 1.333×10^{-2} Pa) for 1 hour. Batching was carried out inside a glovebox under an atmosphere of nitrogen which was continuously recirculated through molecular sieves and over copper turnings, at 110°C, to minimise water and oxygen contamination, respectively. Germanium, sulphur and iodine (supplied by Johnson Matthey) were consecutively weighed to ±0.02% accuracy into the

ampoule, with further degassing under vacuum at each stage at an appropriate temperature before final sealing of the ampoule.

The batched ampoule was loaded into a furnace which was continuously rocked during melting to aid melt homogeneity. The temperature of the furnace was raised to 950°C over a period of 12 h, and maintained at that temperature for ca. 36 h. Melts were air quenched and annealed inside the ampoules for 2 h just below the glass transition temperature (T_g) (see Table 4) and allowed to cool within the annealing furnace. Powder X-ray Diffractometry (XRD) was carried out on the prepared materials using CuK_α radiation. For compositional determination by Energy Dispersive Analysis of X-rays (EDAX), specimens were mounted in epoxy resin, polished to 1 μm and coated with carbon. A Cambridge Instruments CAMSCAN Scanning Electron Microscope and EDS unit were used. Infrared spectroscopy was carried out by means of a Perkin Elmer 683 Spectrophotometer and Data Station PE3600 on specimens which had been polished to a 1 μm finish and had an optical pathlength of a few mm.

Thermal techniques

For both differential scanning calorimetry (DSC) and thermogravimetry (TG), coarse lumps of glass of maximum dimensions 3 mm and total mass about 20 mg were analysed at a heating rate of 10 deg·min^{-1} under an inert atmosphere flowing at 25 cm^3·min^{-1}. The DSC equipment was a Perkin Elmer DSC7 which was calibrated against the melting point of indium. Glass samples were hermetically sealed into aluminium pans with an empty sealed pan as the reference and an argon atmosphere was used. T_g was taken as the extrapolated onset temperature as indicated in Fig. 1. Repeated experiments

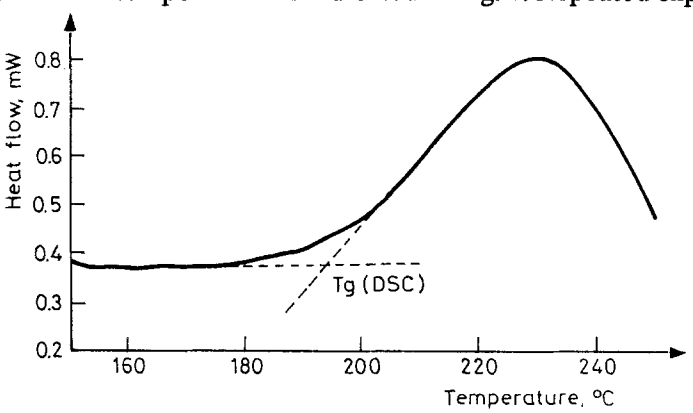

Fig. 1 Differential scanning calorimetry curve of the glass $[Ge_{0.3}S_{0.7}]_{80}I_{20}$ showing the DSC glass transformation temperature

on nominally the same glass composition gave values of T_g/°C which agreed to within ±3% and all DSC runs were terminated just above T_g. The TG equipment was a Stanton Redcroft TG750. The sample was held in an open platinum crucible in a nitrogen atmosphere. The onset of mass loss (T_w) was taken as the temperature at which the baseline first deviated and repeated runs gave values of T_w/°C agreeing to within ±2%.

To measure linear thermal expansion (α), a cylindrical glass sample of length 20–30 mm and 5 mm diameter, with ends ground perpendicular to the length, was placed between silica pusher rods within a silica tube. One end of the rod assembly was restrained and the other was abutted to a linear variable differential transducer (LVDT). To compensate for the expansion of the silica pusher rods another silica rod, also placed within a silica tube and connected to another LVDT, was aligned parallel to the sample rod assembly. The silica tubes were housed in a resistance furnace. Both transducers were interfaced to a Commodore CBM 3032 computer which not only recorded expansion but was also programmed to control the heating rate of the furnace to 5 deg·min^{-1} and terminate the measurement when the specimen began to contract above the dilatometric softening point. Thrice repeated expansion measurements on the same rod, after allowing it to cool slowly in situ, gave α values agreeing to within 3%.

Glass melt viscosities were measured by penetration viscometry using a Dupont Thermal Mechanical Analyser (TMA 943). Verification of the technique using a National Bureau of Standards (NBS) glass, over the range 10^7– $10^{10.7}$ Pas, has been described previously [12]. Absolute viscosities of the chalcogenide-halide glass melts were calculated using an equation derived by numerical fitting of the experimentally determined viscosity/temperature curve of the NBS glass to the NBS Vogel-Fulcher plot. As-annealed cylindrical glass specimens of 8–10 mm diameter and about 3 mm depth were prepared. The larger faces of the specimen were ground parallel to each other to within ±0.05 mm and one face was polished to a 3 μm finish. With the polished face uppermost, a specimen was placed in the TMA cell, on top of a small piece of platinum foil. A 1 mm cylindrical indenter, fabricated inhouse from a high temperature nickel/cobalt/chromium alloy, was placed over the end of the TMA silica probe and supported between the probe and the polished specimen surface. The TMA cell was heated at 100 deg·min^{-1} under nitrogen, flowing at 0.2 dm^3·min^{-1}, to 40° below the required temperature and then at 10 deg·min^{-1} to the set temperature. The isothermal penetration depth was measured as a function of time and measurements were carried out for between 15 and 40 minutes

once a linear penetration rate ensued. Correlation coefficients for the linear response were at least 0.998. After the measurement all specimen surfaces, when examined by means of optical microscopy, appeared defect-free and no specimen underwent mass loss.

Results

From XRD the prepared materials were amorphous (see Fig. 2) and, according to EDAX, all of the Ge-S-I glass composition lay within ±2 at% absolute of those expected as shown in Table 1. Monolithic glass rods up to 30 mm long and 5 mm diameter, and shorter rods of 10 mm diameter, were prepared. A typical infrared spectrum for the glass containing 5% iodine is given in Fig. 3 showing peaks at 2520 and 1135 cm^{-1} due to vibrational absorption of S–H and Ge–O impurities in the glass which arise from un-

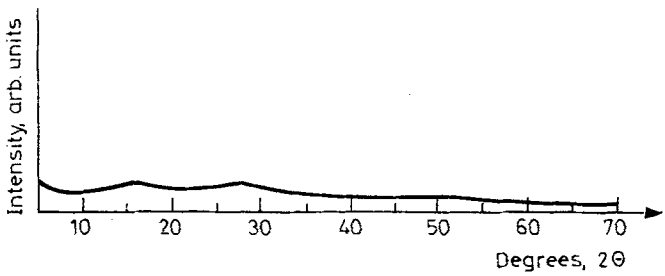

Fig. 2 X-ray diffraction pattern of $[Ge_{0.3}S_{0.7}]_{90}I_{10}$ as prepared showing the amorphous nature

Table 1 Nominal batch compositions of the $[Ge_{0.3}S_{0.7}]_{100-x}I_x$ series of glasses compared to the analysed compositions which were determined by means of Energy Dispersive Analysis of X-rays

Composition / at %					
Nominal			Analysed		
Ge	S	I	Ge	S	I
30.0	70.0	0	30.0	70.0	0
28.5	66.5	5.0	30.1	65.4	4.5
27.0	63.0	10.0	27.0	62.6	10.4
25.5	59.5	15.0	–	–	–
24.0	56.0	20.0	25.8	55.4	18.8
21.0	49.0	30.0	22.1	48.6	29.3

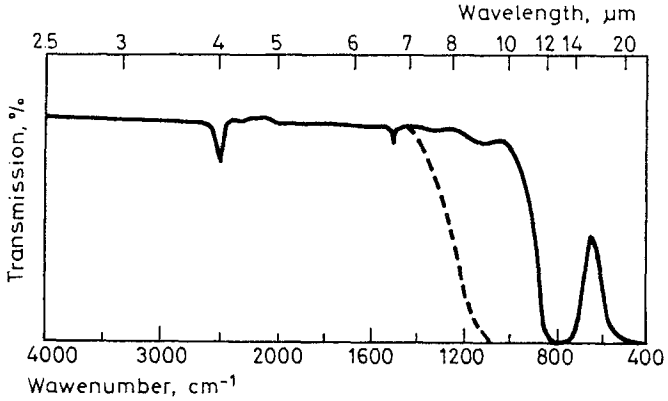

Fig. 3 Infrared spectrum of $[Ge_{0.3}S_{0.7}]_{95}I_5$ of 2–3 mm optical pathlength. Broken line indicates the infrared edge of a ZBLAN glass of similar pathlength

wanted hydrolysis and oxidation during glass melting. Assuming a similar extinction coefficient for Ge–O as for Si–O, we have estimated that oxide contamination approaches 100 ppm. The absorption peak at 1500 cm^{-1} is possibly due to carbon impurities [10]. It is evident from Fig. 3 that the posi-

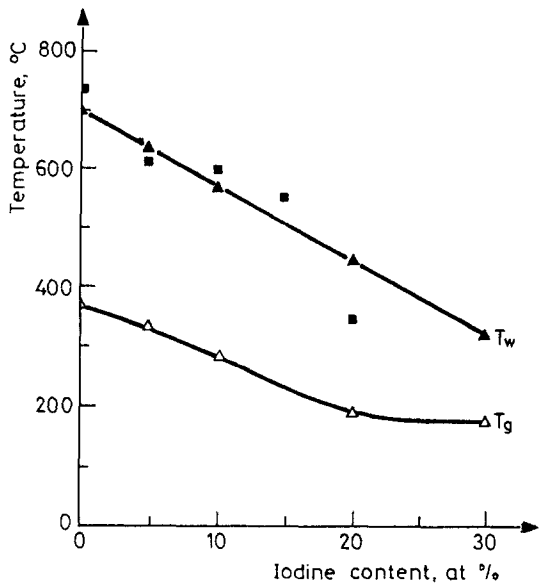

Fig. 4 Variation of the glass transformation temperature found by DSC (T_g), and the temperature of onset of weight loss found by TG (T_w), as the iodine content is raised for the glass series $[Ge_{0.3}S_{0.7}]_{100-x}I_x$. Data points: ■ correspond to the temperature at which glass viscosity is predicted to reach $10^{4.5}$ Pas, i.e. suitable for preform drawing to fibre. These were found by extrapolation of the Vogel-Fulcher fitted curves of data presented in Fig. 5 (see also Table 4)

tion of the infrared edge for the chalcogenide-halide glass is shifted to a longer wavelength relative to that of a ZBLAN specimen of similar path-length.

Figure 4 shows that increasing the iodine content of the Ge–S–I glasses caused a decrease in the DSC T_g. The glasses were found to lose mass on heating and the onset temperature of weight loss (T_w) also decreased with increasing iodine. The $T_w - T_g$ gap, therefore, defines an effective working range of the glasses under these experimental parameters and the gap diminished with increasing iodine. To determine the identity of the volatile species, a sample of glass was placed in an alumina boat partially covered with a microscope slide and held at $T_w + 15°$ under a flowing nitrogen atmosphere. After 10 minutes the boats were withdrawn and quenched to room temperature and the volatile material condensed on the underside of the slide was analysed using EDAX. Analytical errors were about ±5% relative due to interference from the underlying slide. As shown in Table 2 for glasses containing 5 or 20% iodine, the deposits were found to contain over 93% sulphur and ca 5% iodine.

Table 2 Products or volatilisation from $[Ge_{0.3}S_{0.7}]_{100-x}I_x$ glasses close to T_w i.e. the temperature of onset of weight loss as determined by TG

Nominal glass composition / at %			Volatilised product / at %		
Ge	S	I	Ge	S	I
28.5	66.5	5.0	0.1	95.3	4.6
24.0	56.0	20.0	0.4	93.2	6.4

Table 3 Thermal expansion coefficients (α) of $[Ge_{0.3}S_{0.7}]_{100-x}I_x$ glasses and the temperature range of application, together with the dilatometric T_g where this was measurable

x / at %	$\alpha \times 10^6$ / °C	range / °C	Dilatometric T_g / °C
0	14.7	80 – 440	–
5	26.5	80 – 300	315
10	28.2	80 – 260	273
20	68.3	80 – 185	–
30	85.7	80 – 155	–

Thermal expansion coefficients are given in Table 3 averaged over temperature ranges which extend from 80°C, the minimum temperature at which an isochronal heating rate was achieved, to either the softening point or to the increase in slope accompanying T_g prior to the softening point. For

the $GeS_{2.3}$ base glass no deviation due to T_g was found in the expansion curve before softening and α was 14.7×10^{-6} °C^{-1} for 80–440°C. Kawamota and Tsuchihashi [13] similarly noted no curve deviation prior to softening of $GeS_{2.0}$. They determined α for $GeS_{2.0}$ to be 11.5×10^{-6} °C^{-1} for the range 30–440°C and heating rate 3–4.5 deg·min^{-1} and that α increased with increasing sulphur content. T_g was discernible for the 5 and 10% iodine glasses (see Table 3) but was not for the 20 and 30% iodine glasses. Overall, α increased with increasing iodine content for the $[Ge_{0.3}S_{0.7}]_{100-x}I_x$ glass series to the large value of 85.7×10^{-6} °C^{-1} for the 30% I glass.

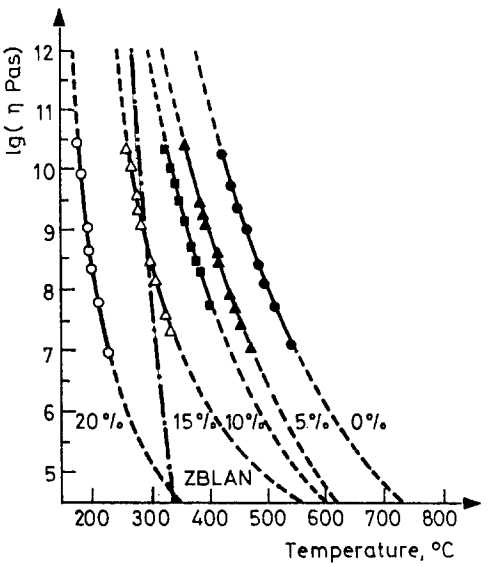

Fig. 5 Viscosity/temperature plots of the $[Ge_{0.3}S_{0.7}]_{100-x}I_x$, where x = 0, 5, 10, 15 and 20 mol%, liquids as determined by penetration viscometry. Broken lines are the extrapolated plots calculated from the Vogel-Fulcher fitting shown in Table 4

Viscosity temperature curves in the range 10^7–$10^{10.7}$ Pas are depicted in Fig. 5. For the Ge–S–I liquids, isoviscous points are found to shift to a lower temperature as the iodine content is increased. The curve for ZBLAN is displayed for comparison and is seen to be significantly steeper than those of the chalcogenide halides.

In general, for optical fibre drawing from a glass preform a viscosity of about $10^{4.5}$ Pas is required at the preform neckdown region. Because of the problems of volatilisation from the Ge–S–I glass melts, the viscosities at the fibre drawing temperatures were not experimentally determined. To obtain a

rough guide of these, we have extrapolated the present viscosity results by fitting to a Vogel-Fulcher curve [14, 15] i.e.:

$$\log_{10}(\eta / \text{Pas}) = A + \frac{B}{T - T_o} \quad (1)$$

where A, B and T_o are material constants and T is temperature in °C. From this the best-fit set of constants for each of the Ge–S–I glasses were calculated using a standard least squares method and are given in Table 4. Although the data were extrapolated over almost three orders of magnitude and the Vogel-Fulcher model was, perhaps, inappropriate especially for the high iodine content glasses, it is interesting to find that the estimated fibre drawing temperatures (Fig. 4) fall above the onset temperature of volatilisation except for the glass containing 20% iodine. Shibata *et al.* [3] have discussed this problem in relation to pulling $GeS_{2.0\text{-}4.0}$ fibres. They used a furnace with a narrow hot zone at the preform neckdown region which would have limited volatilisation by restricting the time that the glass melt was held above T_w. Fibres of $GeS_{2.0\text{-}4.0}$ were coated with silicone resin directly after pulling and this acted as an optical cladding. The silicone resin was subsequently thermally cured at 500°C. When sulphur evolution did occur, irregularities formed at the fibre glass/polymer interface and optical loss of the fibre was substantially increased. From Fig. 4, for Ge–S–I fibres with minimum drawing defects due to volatilisation, it seems advisable to use higher iodine compositions.

Table 4 Vogel-Fulcher parameters (see Eq. (1)) for $[Ge_{0.3}S_{0.7}]_{100-x}I_x$ glass melts determined by least squares fitting of the experimentally measured viscosity/temperature plots shown in Fig. 4, r is the correlation coefficient of the fitted plots with respect to the experimentally measured plots

Iodine content, %	A	B	T_o	r	Vogel-Fulcher Extrapolated T_g / °C
0	–2.4659	4858.1	35.61	0.963	371
5	–3.2831	5689.1	–32.75	0.990	317
10	–1.4356	3282.4	43.64	0.973	288
15	1.8810	1119.4	127.44	0.775	238
20	1.8013	658.1	100.02	0.997	165

The Vogel-Fulcher modelling also gave an estimate for T_g which conventionally is the temperature corresponding to a viscosity of 10^{12} Pas. T_g's, as determined by DSC, generally tend to occur at a viscosity in the range 10^{10}–

$10^{11.5}$ Pas depending on the liquid [16]. Hence agreement here was close but not exact. Where they were observable, the T_g's determined by dilatometry were lower than those determined by DSC but were obtained at a lower heating rate (compare Tables 3 and 4 and Fig. 4).

Discussion

For the Ge-S binary system, Kawamoto and Tsuchihashi [11] found two glass forming regions bound by $GeS_{1.31\text{-}1.50}$ and $Ge\text{-}S_{2.0\text{-}9.0}$. The local structure of $GeS_{2.0}$ glasses was considered to be $\{GeS_4\}$ tetrahedra (T_d) where sulphur is two-fold coordinated by germanium atoms and the structure is analogous to that of SiO_2 with which it is isoelectronic. Lucovsky *et al.* [17, 18] from Raman and infrared spectral studies, drew similar conclusions and suggested that the extended structure was a 3 dimensional network of $\{GeS_4\}$ T_d linked by S bridges. However, later work has shown that the intermediate linking of the $\{GeS_4\}$ tetrahedra in $GeS_{2.0}$ glasses may, instead, be two dimensional [19]. Kawamoto and Kawashima [20] found a striking similarity between vibrational spectral features of vitreous $GeS_{2.0}$ and a crystalline polymorph of GeS_2 which is stable $>500°$ and has a layer structure. For $GeS_{>2.0\text{-}4.0}$ the, excess sulphur is proposed to form $(\text{-S-})_n$ homopolar chains [11], where n is a maximum of 2 according to Lucovsky *et al.* [18], linking neighbouring tetrahedra. For $GeS_{>4.0}$ an increasing amount of S_8 ring molecules were found to be extractable into carbon disulphide and hence it was concluded that S_8 is molecularly dispersed within the matrix in solid solution [11]. Raman spectroscopy supports this conclusion [18, 21].

From vibrational analysis, Heo and Mackenzie [22] have suggested that iodine addition to the germanium sulphide system results in the formation of Ge–I bonds replacing Ge-S bonds within the $\{GeS_4\}$ T_d. Mixed groups of $\{GeI_nS_{4-n}\}$ were identified and S_8 rings or S chains confirmed by characteristic vibrational peaks. Iodine is monovalent and cannot link two Ge atoms like divalent S, thus, as it substitutes sulphur, the overall connectivity of the glassy network is reduced – iodine acts as a network terminator. In addition, the displaced sulphur forms chains to link two Ge atoms or self-polymerises to S_8 molecules. S–S bonds are weaker than Ge-S bonds, hence the overall connective bond strength is lowered. (These structural variations are discussed in greater detail below.)

The thermal behaviour of the $[Ge_{0.3}S_{0.7}]_{100\text{-}x}I_x$ series observed in the present work appears to support this proposed structural variation. T_g's obtained by DSC and other isoviscous temperatures fall as x increases (Figs 4

and 5) and expansion coefficients increase (Table 3) which suggests a weakening of the average bond strength in the network.

As Angell [23] has discussed, by plotting $\log_{10}$ viscosity data on a reduced inverse (absolute) temperature scale (see Figs 6 and 7) it is possible to gain insight on the relative relaxation time of the melt, assuming that this is manifested in the shear viscosity of the liquid. The temperature at which viscosity reaches 10^{12} Pas (T_g) is used as the normalizing parameter.

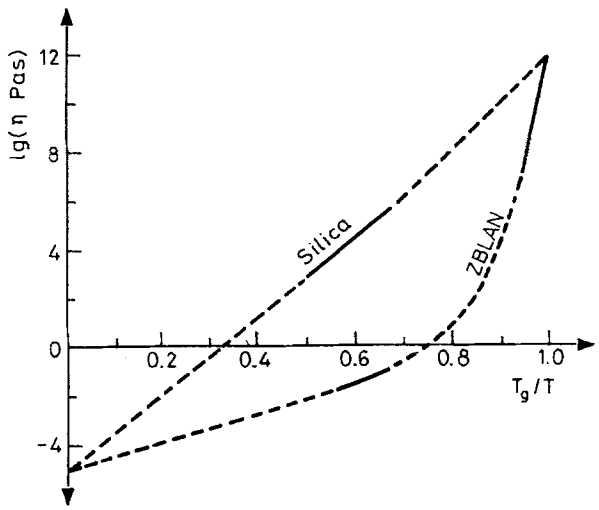

Fig. 6 Viscosity *vs.* reduced temperature relations for silica [23]: a network (Arrhenius) liquid and ZBLAN [24]: an ionic (non-Arrhenius) liquid. Continuous lines represent experimentally determined data

Within this rationale a silica glass melt lies at one extreme of behaviour. Solid vitreous silica has a very strong, mutually supporting, three dimensional covalent network. Above T_g the liquid possesses an almost Arrhenian variation of structural relaxation time which is manifested in a nearly linear scaled viscosity plot; this is termed a strong liquid. Germania glass melts behave similarly. At the other extreme ZBLAN exhibits obviously non-Arrhenian or 'fragile' behaviour, as the melt is predominantly ionic, more weakly bonded and being multicomponent has a range of bond strengths in the liquid. Intermediate fragile structures produce plots between these two extremes for instance Martin and Angell [16] have demonstrated that there is an increasing fragility in progressing from silica to the two dimensional sheer-like structure of network of $Na_2O \cdot 2SiO)_2$ and to the one dimensional chin-like structure of liquid $Na_2O \cdot P_2O_5$. Figure 6 shows the complete scaled

viscosity/temperature plots for silica [16, 23] and ZBLAN melts. Viscosity data for the latter were taken from Hasz *et al.* [24] who have developed a Cohen-Grest type equation to account for the experimental viscosity/temperature behaviour both above and below the crystallization temperature range and hence interpolated viscosities in the crystallization region itself (see Fig. 5). These data have been recalculated against the reduced temperature for Fig. 6.

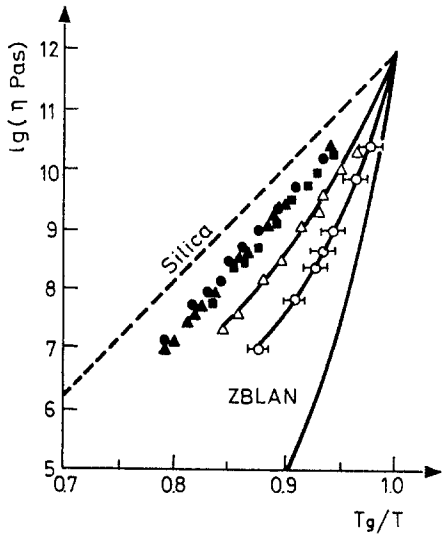

Fig. 7 Viscosity *vs.* reduced temperature relations for $[Ge_{0.3}S_{0.7}]_{100-x}I_x$ liquids showing the progressive fragility as the level of iodine is increased. The horizontal error bars for the 20 mol% iodine melt correspond to an error of ±5 K in the Vogel-Fulcher extrapolated T_g (see Fig. 5 and Table 4). ● - 0% I; ▲ - 5% I; ■ - 10% I; Δ - 15% I; ⊢○⊣ - 20% I.

Figure 7 shows the variation of viscosity data for the $Ge_{0.3}S_{0.7}]_{100-x}I_x$ series on a similarly scaled temperature plot where T_g has been taken as the temperature at which $\eta = 10^{12}$ Pas from the extrapolated Vogel-Fulcher plot as listed in Table 4. The accuracy of the reduced temperature plots is vulnerable to errors in the value taken for the normalizing factor i.e. T_g. The horizontal error bars on the 20 mol% iodine plot in Fig. 7 indicate how an error of ±5 K in the Vogel-Fulcher extrapolated T_g would affect the reduced temperature plot. During the following discussion it is assumed that the errors are not much larger than this.

From Fig. 7 the addition of iodine tends to break down the connectivity of the germanium sulphide network in the melt producing an increasingly fragile liquid. For $0 < x \leq 10$, there is little change with increasing iodine and

these liquids possess a relatively strong network, stronger than the sheet-like structure of $Na_2O \cdot 2SiO_2$ [16]. Further addition of iodine breaks down this structure and there is a large increase in melt fragility for compositions with 15 and 20% iodine.

From Raman and infrared spectroscopy, Heo and Mackenzie [21, 22] were able to describe the progressive disruption of the germanium sulphide lattice in the solid state as the level of halogen incorporated is increased. A detailed comparison was drawn between adding increasing amounts of bromine [21] to base glasses of constant sulphur/germanium ratio: $GeS_{2.0}$ and $GeS_{3.0}$. The authors report that very similar structural variations occurred upon iodine addition [22].

For the series $GeS_{2.0}$, addition of 10% bromine results in tetrahedra of both GeS_4 and mixed GeI_nS_{4-n} ($n = 1$, 2 or 3) with some –S–S– bridges between tetrahedra but no S_8 ring molecules. At 20% bromine, a limited amount of S_8 molecules form (5%) and at 30% halogen there are large numbers of S_8 rings. On the other hand, $GeS_{3.0}$ already contains nonstoichiometric sulphur present mainly as $(–S–)_n$ bridging chains with some S_8 molecules. As halogen is added and substitutes sulphur, then some of the bridging sulphur chains are liberated and self-polymerise to form S_8 rings at a lower threshold bromine concentration than for the $GeS_{2.0}$ series. Heo and Mackenzie [21] detected a rapid increase in S_8 molecules at the 10% bromine composition.

In the current work, the ratio of sulphur to germanium was held at 2.3. Interpolation of Heo and Mackenzie's data means that a rapid increase in S_8 ring molecules should occur between the 10% halogen seen for S:Ge of 2.0 and 20–30% halogen for S:Ge of 3.0. Thus the great increase in glass melt fragility noted here for the 15 and 20% iodine glasses, compared to 0, 5 and 10% I, could be due to a large increase in S_8 molecules dispersed within the matrix.

For the glass $[Ge_{0.3}S_{0.7}]_{80}I_{20}$, the atomic ratio of S:I is 2.8 whereas in the vapour above the glass melt at T_w the ratio is 14.5 (Table 2). This suggests that much of the sulphur in the glass melt is less strongly bound than the iodine. It is likely that the vapour contains sulphur in the S_8 state as these molecules are remarkably stable and are the equilibrium vapour state above crystalline sulphur for temperatures up to 800°C when S_8 begins to break down to S_2 [25]. These results therefore do not contradict the suggestion that the (15 and) 20% I glasses contain dispersed S_8 molecules.

Finally, it is worth noting that oxide contamination of the glasses, estimated earlier to be approaching 100 ppm, may affect physical properties. For instance, assuming no phase separation occurs., for oxygen increasingly

substituting sulphur the reduced viscosity plot of $GeS_{2.3}$ would probably shift towards that shown for SiO_2 in Fig. 7 which nearly superposes that of germania [16].

Conclusions

Chalcogenide-halide glasses in the system $[Ge_{0.3}S_{0.7}]_{100-x}I_x$ where $0 \leq x \leq 30$ have been prepared. As x is increased so the glass transformation temperature, and other isoviscous points in the range $10^7-10^{10.7}$ Pas, decrease and thermal expansion increases indicating a reduction in average bond strength in the network. On a scaled viscosity/temperature plot the glass melts show a large increase in fragility at $x = 15$ and this is tentatively attributed to a large increase in the number of S_8 rings molecularly dispersed in the structure. Fibre drawing temperatures have been estimated and tend to lie very close to the onset temperature of mass loss.

* * *

Financial support for this work from British Telecom Research Laboratories, Martlesham Heath, Ipswich, U.K., in the form of an SERC CASE award for M. A. Hemingway is gratefully acknowledged.

References

1 J. Savage, 'Infrared optical materials and their anti-reflection coatings', Adam Hilger Ltd., Bristol and Boston 1985.
2 T. Katsuyama and H. Matsumura, 'Infrared optical fibres', Adam Hilger, Bristol 1989.
3 S. Shibata, Y. Terunuma and T. Manabe, Mat. Res. Bull., 16 (1982) 703.
4 P. W. France *et al.*, 'Flouride glass optical fibres', Blackie, Glasgow 1990.
5 'Fluoride glasses', Ed. A. E. Comyns, Critical Reports on Applied Chemistry, John Wiley & Sons, Chichester 1989, Vol. 27.
6 H. Nasu and J. D. Mackenzie, Opt. Eng., 26 (1987) 102.
7 A. D. Pearson, Chapter 2 of 'Modern aspects of the vitreous state 3', Ed. J. D. Mackenzie, Butterworths, London 1964.
8 S. A. Dembrovskii, V. V. Kirilenko and Y. Buslaev, Neorg. Matter. Izv. Akad. Nauk USSR, 7 (1971) 328.
9 J. S. Sanghera, J. Heo and J. D. Mackenzie, J. Non-Cryst. Solids, 103 (1988) 155.
10 B. Voigt and M. Wolf, J. Non-Cryst. Solids, 51 (1982) 317.
11 Y. Kawamoto and S. Tsuchihashi, J. Amer. Ceram. Soc., 52 (1969) 626.
12 A. V. Cardoso and A. B. Seddon, 'Penetration viscometry using a Thermal Mechanical analyser', Glass Technology 32 (19911) 103.
13 Y. Kawamoto and S. Tsuchihashi, J. Amer. Ceram. Soc., 54 (1971) 131.
14 H. Vogel, Phys. Z., 22 (1921) 645.
15 G. S. Fulcher, J. Amer. Ceram. Soc., 6 (1925) 339.

16 S. W. Martin and C. A. Angell, J. Phys. Chem., 90 (1986) 6736.
17 G. Lucovsky, J. P. de Neufville and F. L. Galeener, Phys. Rev. B, 9 (1974) 1591.
18 G. Lucovsky, F. L. Galeener, R. C. Keezer, R. H. Geils and H. A. Six, Phys. Rev. B, 10 (1974) 5135.
19 R. Zallen, B. A. Weinstein and M. L. Slade, J. Phys., 42 (1981) 241.
20 Y. Kawamoto and C. Kawashima, Mat. Res. Bull., 17 (1982) 1511.
21 J. Heo and J. D. Mackenzie, J. Non-Cryst. Solids, 113 (1989) 1.
22 J. Heo and J. D. Mackenzie, J. Non-Cryst. Solids, 113 (1989) 246.
23 C. A. Angell, J. Non-Cryst. Solids, 73 (1985) 1.
24 W. C. Hasz, S. N. Crichton and C. T. Moynihan, Mat Sci Forum, 132-33 (1988) 589.
25 N. V. Sidgwick, 'Chemical elements and their compounds', Clarendon Press, Oxford 1950.

Zusammenfassung — Es wurden Chalkogenid-Halogenid-Gläser der Zusammensetzung $[Ge_{0.3}S_{0.7}]_{100-x}I_x$ mit $0 \leq x \leq 30$ hergestellt. Sie besitzen potentielle Anwendungsmöglich-keiten als optische Fasern im kurzen IR-Bereich. Mit der Zunahme von x steigt auch der Ausdehnungskoeffizient. Wie durch DSC und TG ermittelt, nehmen jedoch dabei sowohl die Glasumwandlungstemperatur als auch die Anfangstemperatur des Massenverlustes ab. Die mittels Penetrationsviskosimetrie bestimmten Viskositäten der Schmelze liegen im Bereich 10^7 bis $10^{10.7}$ und durch Ansteigen von x werden isoviskose Punkte in Richtung niedrigerer Temperaturen verschoben. Die Ergebnisse wurden im Hinblick auf bekannte Informationen über die Struktur diskutiert und die Sprödigkeit der Schmelzen miteinander verglichen. Vorausgesagte Faserziehtemperaturen liegen nahe bei den Anfangstemperaturen für den Massenverlust.